J. Biochem. **142,** 421–433 (2007)
doi:10.1093/jb/mvm178

Mechanistic Analysis of the Phosphonate Transition-state Analogue-derived Catalytic and Non-catalytic Antibody

Yoshisuke Nishi[1,*,†], Naoki Yamamoto[2], Kazuko Shimazaki[3], Naoko Takahashi-Ando[1,*], Hiroyuki Kakinuma[1,*], Sun Jialin[1], Sergey N. Ruzheinikov[4], Tatyana A. Muranova[4], David W. Rice[4] and Yasuhiro Kajihara[2]

[1]Laboratory of Life Science & Biomolecular Engineering, Japan Tobacco, Inc., 6-2 Umegaoka, Aoba-ku, Yokohama, Kanagawa 227-8512; [2]Graduate School of Integrated Science, Yokohama City University, 22-2 Seto, Kanazawa-ku, Yokohama, Kanagawa 236-0027; [3]Tobacco Science Research Center, Japan Tobacco, Inc., 6-2 Umegaoka, Aoba-ku, Yokohama, Kanagawa 227-8512, Japan; and [4]Department of Molecular Biology and Biotechnology, Krebs Institute for Biomolecular Research, University of Sheffield, Fifth Court, Western Bank, Sheffield S10 2TN, UK

Received February 1, 2007; accepted May 15, 2007

The esterolytic catalytic antibody (catAb) has the positive charged region interacting with the carbonyl group of the ester substrate. To examine how such a region interacts with the substrate, we compared the catAb with the non-catalytic antibody (non-catAb) for interaction with the non-cleavable amide substrate (a mimic of the ester substrate) and the two end products. Surface plasmon resonance (SPR) analysis revealed that the amide substrate gave the equivalent K_d values for the two antibodies, whereas both the on-rate and off-rate of the catAb were five-times lower than those of the non-catAb. In agreement with SPR analysis, saturation transfer difference (STD) NMR spectroscopy detected the STD signals only between the catAb and one of the product, suggesting the slower exchange rates of the amide substrate in the catAb as compared with the mixing times, whereas it was not the case with the non-catAb. Transferred nuclear Overhauser effect NMR spectroscopy showed the negative signals for only between the non-catAb and the amide substrate or the product, again suggesting the lower off-rates of the catAb as compared with the mixing times. The decreased interaction rates should be the primary consequence of the positively charged region in the combining site in the catAb.

Key words: catAb, saturation transfer difference, surface plasmon resonance, transferred nuclear Overhauser effect NMR spectroscopy.

Abbreviations: TSA, transition-state analogue; EPS, electrostatic potential surface; SPR, surface plasmon resonance; STD, saturation transfer difference; trNOESY, transferred nuclear Overhauser effect spectroscopy; trNOE, transferred nuclear Overhauser effect; ELISA, enzyme-linked immuno sorbent assay.

According to the 'transition-state theory' advocated by Pauling (*1*) and Jencks (*2*), antibodies elicited against stable mimics of a transition-state would catalyse the corresponding reactions. This prediction was first incarnated by successful isolation of esterolytic antibodies among the antibodies having complementary binding to the transition-state analogue (TSA). TSA mimics the tetrahedral structure of the transition-state during ester or amide hydrolysis (*3*, *4*). Dozens of studies proceeded to show the potentials of the TSAs, such as phosphonate, phosphate and phosphonamidate. These TSAs elicit catalytic antibodies (catAbs), which catalyse the hydrolytic reactions of aliphatic esters, aryl esters, carbonate esters, phosphonate esters and amides (*5*).

How such esterolytic catAbs function has been addressed by many studies, including structural analysis with the hapten, studies of homology modelling, reaction kinetics and site-directed mutagenesis (*6–17*). These analyses have shown that catAbs have two binding sites: One is the catalytic site that presents a conserved array of amino acid residues. These residues exhibit an array of hydrogen bond donors complementary to the anion that represents the tetrahedral geometry of the transition-state conformation in the basic hydrolysis of esters and amides (*18*, *19*). The site is held in place at a mouth of the cavity. The other binding site is a hydrophobic pocket that is located at the bottom of the cavity. The residues that form the hydrophobic pocket interact with the end-group (aryl moiety) of the hapten through hydrophobic interactions.

In response to the challenging mice with a phosphonate hapten, we obtained a number of independent esterolytic antibodies. These catAbs are clonally independent but highly related (*20–22*). Recovery of catAbs was more successful with autoimmune MRL/*lpr* mice

*Present addresses: Yoshisuke Nishi, Nagahama Institute of Bio-Science and Technology, 1266 Tamura-cho, Nagahama, Shiga 526-0829, Japan; Naoko Takahashi-Ando, Plant Science Center, RIKEN, 2-1 Hirosawa, Wako, Saitama 351-0198, Japan; Hiroyuki Kakinuma, Medicinary Chemistry Laboratory, Taisho Pharmaceutical Co., Ltd, 1-403 Yoshino-cho, Saitama, Saitama 330-8530, Japan.
†To whom correspondence should be addressed: Tel: +81-749-64-8122, Fax: +81-749-64-8140,
E-mail: y_nishi@nagahama-i-bio.ac.jp

than with normal BALB/c mice. However, the latter challenge yielded a number of antibodies that strongly bound to the hapten (*22–24*). Sequence analyses and 3D studies at the combining sites of the esterolytic antibodies revealed a network of conserved hydrogen bond contacts between the phosphonate TSA and the antibodies (*25*). The 3D results, together with the results of site-directed mutagenesis, indicated that two conserved residues (LysH95 and HisL91) have a catalytic role (*25*). In these antibodies, as in many other antibodies, stabilization of the 'oxy-anion hole', also seems to play a central role of catalytic function. However, the nature and position of the residues in the immediate vicinity of the 'oxy-anion hole' in our catAbs are different from what is observed in other catAbs and these residues were not conserved in the combining site among the non-catalytic binders derived from BALB/c mice (*22–25*).

In our catAbs, a large and strongly positive electrostatic potential surface (EPS) due to a catalytic residue, LysH95, expands around the mouth of hydrophobic pocket that is located at the bottom of the cavity (*23*). Such a positive EPS should interact not only with the TSA, but also with the substrate, when the substrate is in the ground-state and its products, before it functions to stabilize the tetrahedral transition-state structures of the substrate. If the positive EPS does interact with the substrate, it should influence the on-rate and/or off-rate with which the ester/amide substrates and their products bind to and unbind from the catAbs. For non-catAbs, *i.e*. these without catalytic residues, would be expected to interact with the substrates and products much less strongly than the catAbs. In order for an antibody to function as a catAb, it might require a positive EPS to interact with the substrate, and without this interaction it cannot be a catalyst, even if it has strong affinity for the TSA. We have been interested in determining whether such an interaction really has a role in catalytic reactions. In order to address this question, we investigated the modes by which catAbs bind to the substrate and products and compared them with those for a typical non-catalytic antibody.

We used the esterolytic catAb with high catalytic activity and a non-catAb. Both antibodies showed a strong binding affinity for the TSA. To observe the interaction modes, we used surface plasmon resonance (SPR) analysis and NMR spectroscopic analyses, saturation transfer difference (STD), NMR spectroscopy (*26–33*) and 2D transferred nuclear Overhauser effect spectroscopy (trNOESY) (*34–44*).

MATERIALS AND METHODS

Antibody preparations—The antibody preparations used in this experiment are MS6-164 and BS6-16. MS6-164 is an esterolytic antibody that cleaves the ester substrate (**1**) into Product-A (phenylalanine) (**2**) and Product-B (phenethylamine) (**3**) (Fig. 1A) and the BS6-16 is an antibody that did not cleave the ester substrate (**1**) (*45*). The MS6-164 was isolated from a hybridoma obtained from the autoimmune strain MRL-MPJ-*lpr*/*lpr* and the BS6-16 from the normal

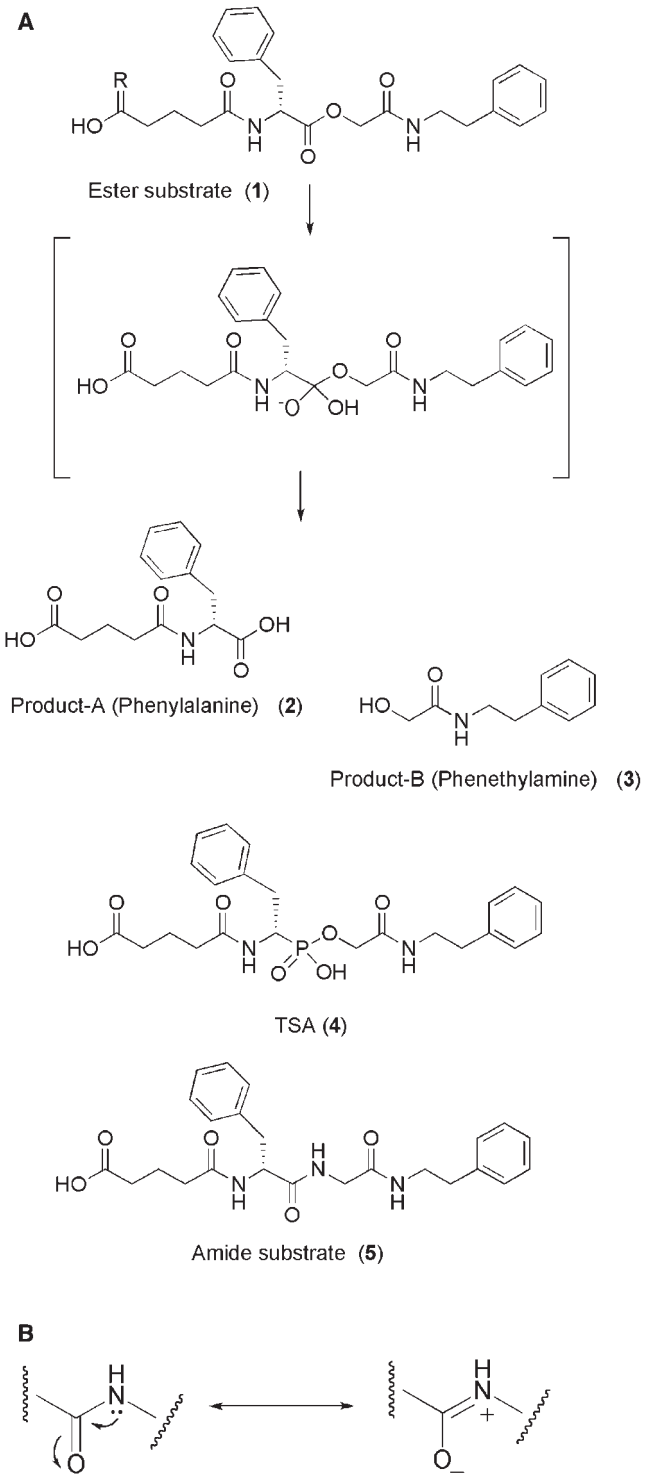

Fig. 1. **Esterase reaction and structural formula of substrate, products, amide substrate and transition-state analogue (A) and resonance structure of amide (B).**

strain BALB/c after the mice were immunized with a TSA (**4**) linked with a linker sequence and keyhole lympet hemocyanin (*45*). ELISA experiments showed that both MS6-164 and BS6-16 had strong affinity towards TSA (**4**) (K_d was 0.61 nM for MS6-164 and

A. V_H sequences:

```
         1                              30  CDR1   36           49        CDR2
MS6-164: QVQLQQPGAELVKPGASVKLSCKASGYTFT SNWIN   WVKQRPGQGLEWIG NIYPDSYRTNYNEKFKR
BS6-16:  D----ES-PG----SQ-LS-T-TVT--SI- -AYAWN  -IR-F--DK---M- Y-RFSGTTSYNPSLKS

         66                             94    CDR3    103       113
         KATLTVDTSSSTAYMQLSSLTSDDSAVYYCVR KHYSYDGVVY WGQGTLVTVSA
         RISI-R---KNQFFL-QLNSVTTEDTAT-YCA LPG        -----------
```

B. V_L sequences:

```
         1                      23        CDR1        35            49   CDR2
MS6-164: DIVMTQAAPSVSVTPGESVSISC RSSKSLLHSNGNTYLY WFLQRPGQSPQLLIY RMSNLAS
BS6-16:  QA-V--ESALTTSPG-TVILTC  ---TGAVTTSNYAN    -VQEK-DHLFTG--G GT---A-

         57                             88    CDR3   98       107
         GVPDRFSGSGSGTDFTLRISRVEAEDVGVYYC LQHLEYPFT FGAGTKLELK
         ---V-----LI-DKAA-T-TGAQT--DAM-F- ALWYSTH-V Ð-G---VTVLG
```

Fig. 2. **Amino acid sequences of variable regions of MS6-16 and BS6-16 antibodies.**

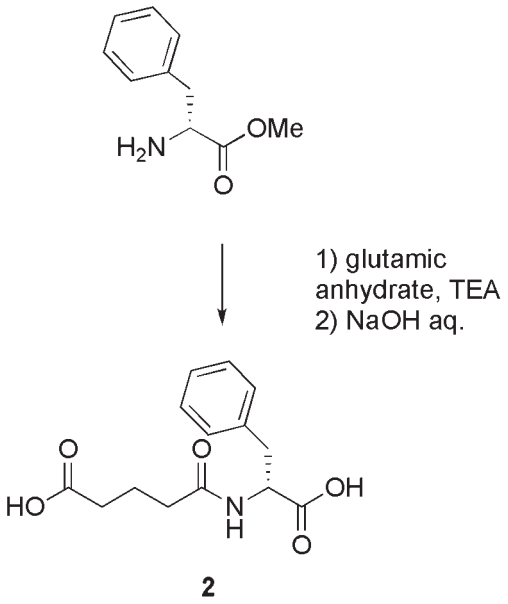

2

Fig. 3. **Synthesis of Product-A (Phenylalanine) 2.**

0.07 nM for BS6-16) (*22*). The sequences of variable regions of MS6-164 and BS6-16 are shown in Fig. 2. Isolation of hybridomas and preparation of antibodies and crystallization were as previously described (*20*, *21*, *45*, *46*).

Chemical Synthesis—Synthesis of Product-A (**2**) (Fig. 3) To a solution of D-phenylalanine (OMe) (20 mg, 0.11 mmol) in CH_2Cl_2 (1 ml) was added glutaric anhydrate (18 mg, 0.15 mmol) and triethylamine (22 mg, 0.22 mmol). This mixture was stirred at room temperature. After the reaction was completed, the mixture was washed with 1M HCl solution and brine and then organic layer was dried with $MgSO_4$. This organic solution was concentrated *in vacuo*. Then, the residue was treated with sodium hydroxide and this mixture was stirred at room temperature. After the reaction was completed, the mixture was neutralized with IR-120 (+) and concentrated *in vacuo*. Purification of the residue was performed by preparative TLC (EtOAc:MeOH = 3:1) that could afford **2** (70%, 20 mg). [Found: ^{1}H-NMR(400 MHz, D_2O) δ 7.46–7.34 (m, 5H), 4.61 (dd, J = 9.59, 4.62 Hz, 1H), 3.32 (dd, J = 13.9, 4.62 Hz, 1H), 2.98 (dd, J = 13.9, 9.59 Hz, 1H), 2.29 (m, 2H), 2.16 (m 2H), 1.77 (m, 2H)].

Synthesis of biotinylated Product-A with a linker (**8**) (Fig. 4)

To a solution of phenylalanine amido substrate (**6**) (20 mg, 45 μmol) in DMF (400 μl) was added *N*-hydroxy succinimide (8 mg, 52.5 μmol) and dicyclohexylcarbodiimide (14 mg, 52.5 μmol) and this solution was stirred at room temperature under argon atmosphere. After 4h, the mixture was filtered and the filtrate was concentrated *in vacuo*. To a solution of the residue in DMF (400 μl) was added triethylamine (10 μl, 52.5 μmol) and 2-aminoethanethiol (6 mg, 52.5 μmol). And this mixture was stirred at room temperature under argon atmosphere. After 30 min, the mixture was concentrated *in vacuo*. Purification of this residue was performed by preparative TLC (EtOAc:MeOH = 3:1) that could afford **7** (63%, 13 mg) [Found: ^{1}H-NMR(400 MHz, $CDCl_3$) δ 7.26–7.01 (m, 5H), 4.88 (m, 1H), 3.70 (s, 3H), 3.41 (m, 1H), 3.22 (m, 1H), 3.08 (dd, J = 5.45, 13.4 Hz, 1H), 3.01 (dd, J = 6.44, 13.4 Hz, 1H),

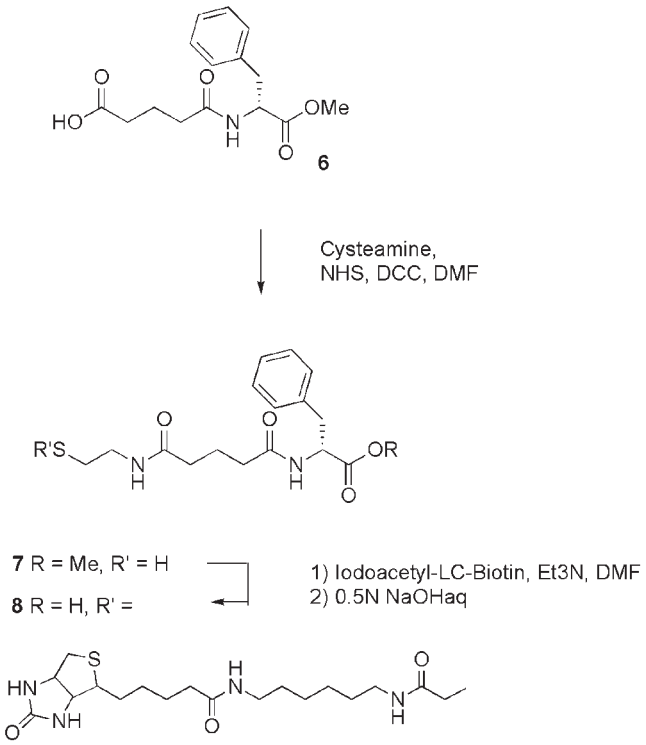

Fig. 4. **Synthesis of biotinylated Product-A (Phenylalanine) with a linker 8.**

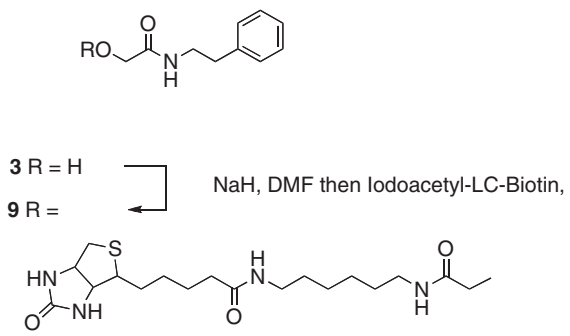

Fig. 5. **Synthesis of biotinylated Product-B (Phenethylamine) 9.**

2.65–2.48 (m, 2H), 2.23–2.02 (m, 4H), 1.88 (m, 2H); HRMS Calcd for $C_{17}H_{24}N_2NaO_4S$ [M + H$^+$] 353.1535, found 353.1542].

To a solution of **7** (3 mg, 6 μmol) in degassed DMF (100 ml) was added iodoacetyl-LC- Biotin (PIERCE: 2.5 mg, 4.9 μmol) and triethylamine (2 μl, 14 μmol) and then this mixture was stirred at room temperature under argon atmosphere. After 4 h, the mixture was concentrated *in vacuo*. Purification of the residue was performed by preparative TLC (EtOAc:MeOH = 3:1) that could afford **8** (65%, 3.4 mg) [Found: ^{1}H-NMR(400 MHz, CD_3OD) δ 7.27–7.14 (m, 5H), 4.60 (dd, J = 4.73, 8.42 Hz, 1H), 4.49 (dd, J = 4.74, 7.90 Hz, 1H), 4.30 (dd, J = 4.74, 7.90 Hz, 1H), 3.38 (m, 2H), 3.26–3.12 (m, 6H), 2.95 (dd, J = 8.42, 13.4 Hz, 1H), 2.93 (dd, J = 4.73, 12.9 Hz, 1H), 2.70 (d, J = 13.4 Hz, 1H), 2.70 (*t*, J = 6.58 Hz, 2H), 2.21–2.16 (m, 4H), 2.11 (*t*, J = 7.37 Hz, 2H), 1.82 (m, 2H), 1.77–1.29 (m, 16H); HRMS Calcd for $C_{34}H_{52}N_6NaO_7S_2$[M + Na$^+$] 743.3237, found 743.3249].

Synthesis of biotinylated Product-B (**9**) (Fig. 5)

To a solution of **3** (10 mg, 60 μmol) in DMF (500 μl) was added NaH (1.3 mg, 60 μmol) and the mixture was stirred at room temperature under argon atmosphere. After 1 h, to this mixture was added iodoacetyl-LC-Biotin (PIERCE: 10 mg, 20 μmol) and the mixture was stirred at room temperature. After 4 h, to this mixture was added MeOH to quench the reaction and the mixture was neutralized with acetic acid. After concentration of this mixture *in vacuo*, purification of the residue was performed by preparative TLC (EtOAc:MeOH = 3:1) that could afford **9** (14 mg, 43%) [Found: ^{1}H-NMR(400 MHz, CD_3OD) δ 7.29–7.16 (m, 5H), 4.47 (dd, J = 4.73, 8.41 Hz, 1H), 4.28 (dd, J = 4.73, 8.41 Hz, 1H), 4.00 (s, 2H), 3.98 (s, 2H), 3.47 (*t*, J = 7.36 Hz, 2H), 3.25–3.14 (m, 5H), 2.91 (dd, J = 4.73, 12.6 Hz, 1H), 2.82 (*t*, J = 7.36 Hz, 2H), 2.69 (d, J = 12.6 Hz 1H), 2.18 (*t*, J = 7.36 Hz, 2H), 1.77–1.25 (m, 14H); HRMS Calcd for $C_{28}H_{43}N_5NaO_5S$ [M + Na$^+$] 584.2883, found 584.2884].

Synthesis of TSA (**4**)

Synthesis of **4** is previously described (*26*). The data of NMR are also shown (*26*).

Synthesis of amido substrate (**5**) and biotinylated substrate (**12**) (Fig. 6)

For synthesis of **5**, to a solution of Z-D-Phenylalanine (50 mg, 0.17 mmol) and glycyl-2- phenethylamine hydrochloride (**10**) (54 mg, 0.25 mmol) in CH_2Cl_2 (1 ml) were added EDC (38 mg, 0.18 mmol) and triethylamine (34 mg, 0.34 mmol). This mixture was stirred at room temperature. After the reaction was completed, the mixture was diluted with CH_2Cl_2 and this organic layer was washed with 1M hydrogensulfate, aq$NaHCO_3$ and brine. The organic layer was dried with $MgSO_4$ and then concentrated *in vacuo*. To a solution of the residue in MeOH (1 ml) was added 10% Pd/C and the mixture was stirred under H_2 atmosphere. After finishing the reaction, the mixture was filtered with a Celite pad and the filtrate was concentrated *in vacuo*. To a solution of the residue in CH_2CL_2 (1 ml) was added triethylamine (34 mg, 0.34 mmol) and glutaric anhydride (29 mg, 0.25 mmol). This mixture was stirred at room temperature. The mixture was washed with 1M HCl solution and brine and then organic layer was dried with $MgSO_4$. This organic solution was concentrated *in vacuo*. Purification of the residue was performed by silica gel column (Hex:EtOAc = 1:10) that could afford **5** in 75% (56 mg) [Found: ^{1}H-NMR(400 MHz, CD_3OD) δ 7.29–7.14 (m, 10H), 4.47 (dd, J = 6.46, 8.69 Hz, 1H), 3.84 (d, J = 16.7 Hz, 1H), 3.61 (d, J = 16.7 Hz, 1H), 3.39 (*t*, J = 7.57 Hz, 2H), 3.13 (dd, J = 6.46, 13.6 Hz, 1H), 2.91 (dd, J = 8.69, 13.6 Hz, 1H), 2.79 (*t*, J = 7.57 Hz, 2H), 2.23 (*t*, J = 7.57 Hz, 2H), 2.21 (*t*, J = 7.57 Hz, 2H), 1.79 (m, 2H)].

For the synthesis of **12**, to a solution of **5** (20 mg, 45 μmol) in DMF (400 μl) was added *N*-hydroxy succinimide (8 mg, 52.5 μmol) and dicyclohexylcarbodiimide

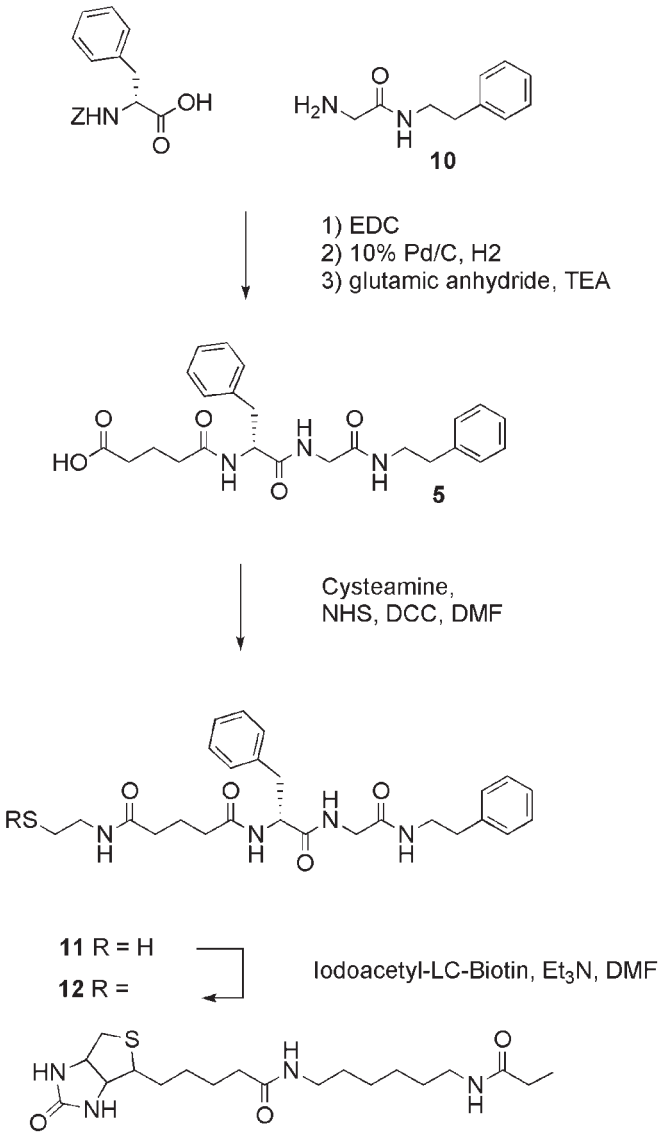

Fig. 6. **Synthesis of amide substrate 5 and biotinylated substrate 12.**

(14 mg, 52.5 μmol). This solution was stirred at room temperature under argon atmosphere. After 30 min, the mixture was concentrated *in vacuo*. Purification of this residue was performed by preparative TLC (EtOAc:MeOH = 3:1) that could afford **11** (63%, 13 mg) [Found: ^{1}H-NMR(400 MHz, CD_3OD) δ 7.30–7.13 (m, 10H), 4.48 (dd, J = 6.56, 8.74 Hz, 1H), 3.85 (d, J = 16.6 Hz, 1H), 3.61 (d, J = 16.6 Hz, 1H), 3.39 (*t*, J = 7.48 Hz, 2H), 3.29 (m, 2H), 3.13 (dd, J = 6.51, 14.0 Hz, 1H), 2.91 (dd, J = 8.78 Hz, 1H), 2.79 (*t*, J = 7.81 Hz, 2H), 2.57 (*t*, J = 7.16 Hz, 2H), 2.21 (*t*, J = 7.48 Hz, 2H), 2.12 (m, 2H), 1.82 (m, 2H); HRMS Calcd for $C_{26}H_{34}N_4NaO_4S$[M + Na^+] 521.2199, found 521.2232].

To a solution of **11** (3 mg, 6 μmol) in degassed DMF (100 ml) was added iodoacetyl-LC- Biotin (PIERCE: 2.5 mg, 4.9 μmol) and triethylamine (2 μl, 14 μmol) and then this mixture was stirred at room temperature under argon atmosphere. After 4 h, the mixture was concentrated *in vacuo*. Purification of the residue was performed by preparative TLC (EtOAc:MeOH = 3:1) that could afford **12** (65%, 3.4 mg) [Found: ^{1}H-NMR (400 MHz, CD_3OD) δ 7.29–7.17 (m, 10H), 4.51–4.45 (m,2H), 4.28 (dd, J = 5.07, 7.97 Hz, 1H), 3.85 (d, J = 16.6 Hz, 1H), 3.62 (d, J = 16.6 Hz, 1H), 3.41–3.33 (m, 4H), 3.21–3.10 (m, 6H), 2.92 (m, 2H), 2.79 (*t*, J = 7.97 Hz, 2H), 2.69 (m, 3H), 2.22 (*t*, J = 7.24 Hz, 2H), 2.18 (*t*, J = 7.24 Hz, 2H), 2.12 (*t*, J = 7.24 Hz, 2H), 1.82 (m, 2H), 1.77– 1.28 (m, 16H); HRMS Calcd for $C_{44}H_{64}N_8NaO_7S_2$[M + Na^+] 903.4237, found 903.4276].

SPR analysis—Kinetic parameters, K_d, k_{on} and k_{off}, of MS6-164 and BS6-16 and amide substrate 5, Product-A (2), Product-B (3) and TSA (4) were analysed by a BIAcore 1,000 analyser (BIAcore, Sweden). Kinetic measurements were calculated from the sensorgrams with BIAevaluation software, version 3.0 (BIAcore), according to the global fitting model. The response curves with various analyte (antibody) concentrations were globally fitted to a bivalent analyte model, in which the first step, A + B ⇌ AB, and the second step, AB + B ⇌ AB2, where A is a concentration of analyte, and B is a concentration of ligand at t = 0. All experiments were performed at 25°C in a running solution (10 mM Tris buffer, 150 mM NaCl and 5 mM EDTA at pH 7.6) at 0.41, 0.83, 1.66 and 3.33 μM for MS6-164 and 0.24, 0.48, 0.96 and 1.92 μM for BS6-16, respectively. The streptavidin chip (SA5, BIAcore) in the flow cells has a gold surface to which a carboxymethylated dextran layer is bound. The dextran layer was activated to bind streptavidin following the user's protocol of the manufacturer. Prior to the experiments, the streptavidin surface was cleaned three times with a solution of 0.05 N NaOH/1M NaCl for 1min in each cleaning. For the SPR assays, biotinylated amide substrate (**12**), Product-A with a linker (**8**) and Product-B (**9**) (each, 0.016 μg/ml) were used as a ligand. These compounds in the running buffer were then added up to 4 resonance units for (**12**) and the maximum amount for (**8**) and (**9**) on the surface of the streptavidin chip to immobilize through a biotin–streptavidin interaction. For TSA (**4**), the maximum amount was directly linked to the amino groups of the surface of the chip following the manufacturer's protocol. And in each experiment, the BIAcore system was cleaned to remove any residual detergents or absorbed proteins in the system following the protocol recommended by the manufacture.

NMR Experiments—The NMR experiments were performed on a Bruker Advance DMX500 spectrometer (Bruker Biospin GmbH, Rheinstetten, Germany). All spectra were acquired at 298 K without sample spinning and HDO signal was used as an internal reference (4.81 p.p.m. at 298 K). XWINNMR software (Bruker) running on a Silicon Graphics workstation was used for data acquisition and processing. Fab fragments, which were used for NMR experiments, were prepared from the corresponding IgG by treatment with papain following the conventional procedure.

STD NMR Spectroscopy—STD NMR spectroscopy experiments were performed according to the previous reports (Mayer and Meyer, 1999; Mayer and Meyer, 2001).

The saturation filed (20–50 Hz) was applied at different frequencies ranging from –0.5 p.p.m. up to 8.5 p.p.m. of the protein spectrum, among which the ligand signals did not overlap with the protein. The spectra were acquired in the direct difference mode: scan at saturation on-resonance (MS6-164:384.7 Hz, BS6-16:450.0 Hz) minus scan at saturation off-resonance (6,566 Hz), with a total of 512 scans per spectrum using CYCLOP phase-cycling. Saturation times varied from 50 ms to 1.2 s. Each sample contained 1 mg of Fabs (MS6-164 and BS6-16) and the ligands [amide substrate (**5**), Product-A (**2**) and Product-B (**3**)] at 20 equivalents of each Fab in 250 μl of the buffer solution (100 mM deuterized sodium phosphate buffer, pH 7.0), thus the final concentration was 80 μM for Fab (50 kDa) and 1.6 mM for the ligands. The samples were assayed either in the absence or presence of an equivalent concentration of (80 μM) of TSA (**4**).

TrNOESY—Pulse sequence of trNOE used in this experiment followed the standard Bruker program, noesytppr. A total of 256 ($t1$)–4 K ($t2$) data points were recorded for each experiment. Prior to Fourier transformation, the data matrix was multiplied with a squared cosine function. The spectral width was 16.0 p.p.m. The HDO signal was suppressed by low-power pre-saturation during the relaxation and mixing time. The total relaxation delay was 1.5 s. Mixing times of 100–600 ms were used. Thirty-two dummy scans and 16 scans per increment were performed. Each sample contained the same concentrations of Fabs and the ligands in 250 μl of the buffer solution (100 mM deuterized sodium phosphate buffer, pH 7.0).

X-ray crystallography—X-ray crystallography was previously performed following the crystals of Fab fragment of MS6-164 and TSA (**4**) using the hanging drop vapour-diffusion method (*25*, *46*). The semi-transparent solvent accessible (1.4 Å probe radius) surface of the Fab structure as seen in its binary complex with TSA (4) (Web Lab Viewer Pro4.0 representation) coloured according to the electrostatic potential with the TSA (4) molecule shown in the active site of the catalytic antibody MS6-164. The only protein atoms were included in the surface calculation.

RESULTS

Kinetic parameters determined by SPR analysis—The binding ability of antibodies to the ligand is expressed as K_d, which can be measured as the ratio of off-rate (k_{off})/on-rate (k_{on}) of the ligand to the antibody. In the present experiment, we used SPR analyses and measured these values for the substrate and the products. We used a biotinylated amide substrate (**12**) as a non-cleavable amide substrate (**5**), instead of a cleavable ester substrate (**1**). We also used a biotinylated Product-A with a linker (**8**) and a biotinylated Product-B (**9**). The amide substrate (**5**) can show resonance structures around the amide bond (Fig. 1B) and it well reproduces the atmosphere of negative charge around the oxy anion of the carbonyl moiety of the ester substrate (**1**).

The K_d values of the catAb MS6-164 for the amide substrate (**5**) (11.7 μM) was similar to that of the non-catAb BS6-16 (11.3 μM) (Table 1). The on- and off-rates of amide substrate (**5**) were different for MS6-164 and BS6-16. The on- and off-rate constants of amide substrate (**5**) for MS6-164 ($k_{on} = 5{,}320\ M^{-1}s^{-1}$ and $k_{off} = 0.0625\ s^{-1}$, respectively) were both about 1/5 of those for BS6-16 antibody ($k_{on} = 28{,}900\ M^{-1}s^{-1}$ and $k_{off} = 0.328\ s^{-1}$). These results demonstrate that amide substrate (**5**) is held longer in the combining site of MS6-164 antibody than in that of BS6-16 antibody. We could not obtain measurable data for either product [Product-A (**2**) or Product-B (**3**)] or TSA (**4**) (data not shown). The former was probably because the affinities were too low, whereas the latter was too high for the SPR analysis using the BIAcore system.

Table 1. **Dissociation parameters (K_d, K_{on} and K_{off}) towards amide substrate (5).**

	K_d (μM)	K_{on}(1/Ms)	K_{off} (1/s)
MS6-164	11.7 [1.0]	5320 [1.0]	0.0625 [1.0]
BS6-16	11.3 [1.0]	28900 [5.4]	0.328 [5.2]

The values in square parenthesis indicate relative incidence.

STD NMR Spectroscopy—As the SPR analyses failed to provide direct evidence of interaction between either antibody or the products [Product-A (**2**) and Product-B (**3**)] and TSA (**4**), we attempted to detect these interactions with STD NMR spectroscopy experiments.

STD NMR spectroscopy is well suited for identifying the compound of the ligand that binds to the protein. The component of the ligand that has the strongest contact to the protein will give the most intense NMR signal, which makes it possible to map of the ligand's binding epitope. In this method, the protein resonances are first selectively saturated by pulse irradiation without affecting the ligand's resonances. This saturation is spread over the entire protein by intramolecular saturation transfer (spin diffusion). Only the ligands interacting with the proteins are saturated by intramolecular saturation transfer. Through the chemical exchange between the free and bound states, these saturated ligands are transferred into solution, in which their ^{1}H signals are detected. A fast-exchange equilibrium of ligands between the bound- and free-states is required to detect a ligand molecule in solution (*28*).

We acquired STD NMR spectra for interactions between each of the antibodies (MS6-164 or BS6-16) and each of the ligands [amide substrate (**5**), Product-A (**2**) or Product-B (**3**)]. The molar concentration ratios for ligand versus antibody were set 20:1 and the saturation times were set for 50–1,200 ms. The data are shown as plus, if the STD spectrum was observed (Table 2). The parent 1D ^{1}H NMR of Product-B (**3**) in the presence of MS6-164 antibody and that of Product-B (**3**) in the presence of BS6-16 antibody are shown in Figs. 7A and 8A, respectively. Example spectra, both made with saturation times of 1,000 ms, are shown for the interactions between Product-B (**3**) and MS6-164 (Fig. 7B) and between Product-B (**3**) and BS6-16 (Fig. 8B). Addition of TSA (**4**) to the solutions of each of the antibodies (MS6-164 and BS6-16) and each of the ligands [amide substrate (**5**) or Product-B (**3**)] quenched the STD signals (Fig. 7C, Fig. 8C and Table 2).Both the 1D ^{1}H reference

Table 2. **STD signals on different saturation times**

Ligand/Antibody	Saturation time (ms)									
	50	100	200	300	400	500	600	800	1000	1000[a]
Amide substrate (**5**)/MS6-164	–	–	–	–	–	–	–	–	–	NE[b]
Amide substrate (**5**)/BS6-16	–	–	–	–	+	+	+	+	+	–
Product-A (**2**)/MS6-164	NE[b]	NE[b]	–	NE[b]	NE[b]	–	NE[b]	–	–	NE[b]
Product-A (**2**)/BS6-16	NE[b]	NE[b]	–	NE[b]	NE[b]	–	NE[b]	–	–	NE[b]
Product-B (**3**)/MS6-164	–	–	–	–	+	+	+	+	+[c]	–[c]
Product-B (**3**)/BS6-16	–	–	–	–	+	NE[b]	+	+	+[d]	–[d]

[a]STD experiments in the presence of TSA (**4**). [b]NE, not examined. [c]Experimental data are shown in Fig. 7. [d]Experimental data are shown in Fig. 8.

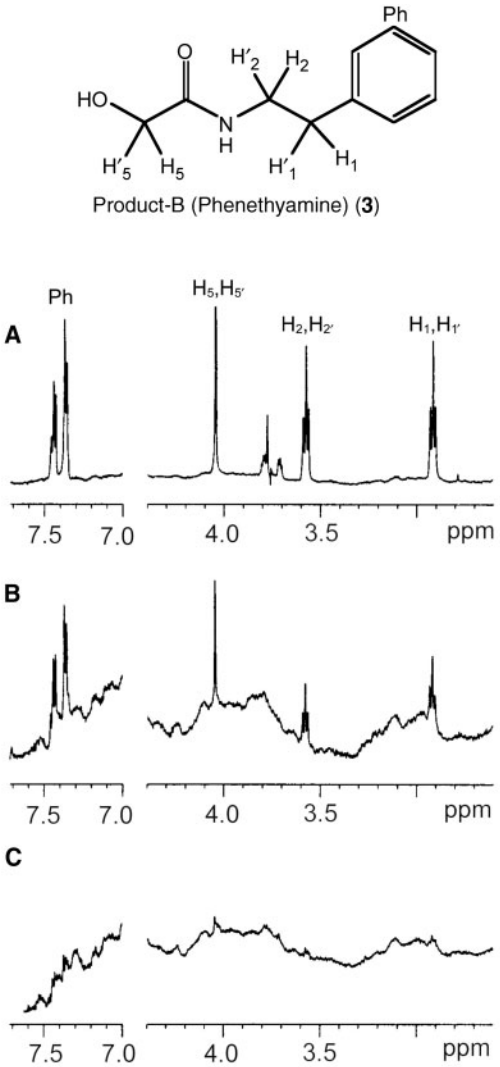

Fig. 7. **Interaction of Product-B (3) and esterolytic antibody MS6-164.** (**A**) 1D ^{1}H NMR spectrum of Product-B (**3**) and MS6-164. (**B**) STD spectrum of Product-B (**3**) and MS6-164. The spectrum was obtained at saturation time of 1,000 ms. (**C**) STD spectrum of Product-B (**3**) and MS6-164 in the presence of 80 μM of TSA **4** equivalent to the final concentration of Fab. The spectrum was obtained at saturation time of 1,000 ms.

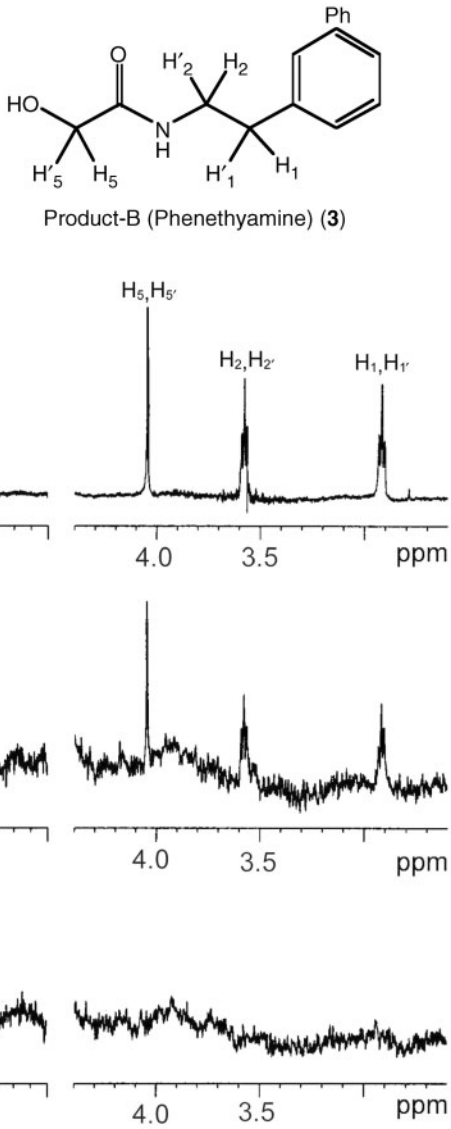

Fig. 8. **Interaction of Product-B (3) and non-catalytic antibody BS6-16.** (**A**) 1D ^{1}H NMR spectrum of Product-B (**3**) and BS6-16. (**B**) STD spectrum of Product-B (**3**) and BS6-16. The spectrum was obtained at saturation time of 1,000 ms. (**C**) STD spectrum of Product-B (**3**) and BS6-16 in the presence of 80 μM of TSA **4** equivalent to the final concentration of Fab. The spectrum was obtained at saturation time of 1,000 ms.

NMR spectrum of Fig. 7A and the STD NMR spectrum of Fig. 7B clearly show that Product-B (**3**) specifically binds to MS6-164 antibody. In this binding, almost all moieties of Product-B (**3**) rather evenly interact with the combining site of MS6-164, because several groups [the terminal phenyl group (Ph), methylene groups neighbouring the phenyl group (H_1, H'_1 and H_2, H'_2), and terminal methylene groups (H_5, H'_5)] gave large proton signals in the STD spectrum at saturation times more than 400 ms. These signals were identical to those in the 1D ^{1}H reference spectrum of Product-B (**3**).

The binding signals were completely abolished by the addition of TSA (**4**) (Fig. 7C) This observation leads us to conclude that Product-B (**3**) competitively binds to the combining site in the presence of TSA (**4**). MS6-164 antibody bound much more weakly to Product-B (**3**) than to TSA (**4**). A similar result was obtained in the case of BS6-16 antibody. All moieties of Product-B (**3**) interact with the combining site of BS6-16 antibody. The binding signals were also completely abolished by adding TSA (**4**). This suggests that the binding of BS6-16 to Product-B (**3**) is structure-specific and that BS6-16 binds to Product-B (**3**) more weakly than BS6-16 binds to TSA (**4**).

STD NMR spectra of Product-A (**2**) and MS6-164 antibody or of BS6-16 antibody did not give significant proton signals up to a saturation time interval of 1,000 ms (Table 2). So, the interactions between Product-A (**2**) and MS6-164 or BS6-16 antibodies were negligible or less than the detectable limit.

Different results were observed between the STD NMR spectra of amide substrate (**5**) and MS6-164 antibody and of amide substrate (**5**) and BS6-16 antibody (Table 2). In the former interaction, there were no meaningful proton signals large enough to be identical to those of the 1D ^{1}H reference spectrum of amide substrate (**5**), even up to the longest saturation time of 1,200 ms (Table 2). In the latter interaction, however, there were large signals identical to those acquired in the 1D ^{1}H spectrum of amide substrate (**5**) after a saturation time of 400 ms. Addition of TSA (**4**) to the sample containing amide substrate (**5**) and BS6-16 abolished the STD signals of amide substrate (**5**) and BS6-16. This effect of TSA (**4**) shows the specific interaction with amide substrate (**5**) and BS6-16 antibody.

For the former case, our understanding is that it does not mean the negligible or weakest interaction between amide substrate (**5**) and MS6-164 antibody, but rather the too much slow exchange rate of amide substrate (**5**) from bound- to free-state, or from free- to bound-state, or both. This argument is further discussed later. The above results also showed that the combining sites of MS6-164 and BS6-16 antibodies are specific for the structure of TSA (**4**).

TrNOESY—TrNOESY can provide insights into the conformational properties of small molecules (or ligands) in the combining site of the receptor proteins. It also provides a way to identify molecules from a mixture of compounds each having binding affinity for a protein (*40*). Small molecules (MW < 1.5 kDa) in the free-state yield small, positive NOEs, while large molecules, *e.g.* proteins with MWs larger than 10 kDa, yield large and negative NOEs. Ligands that reversibly bind to a

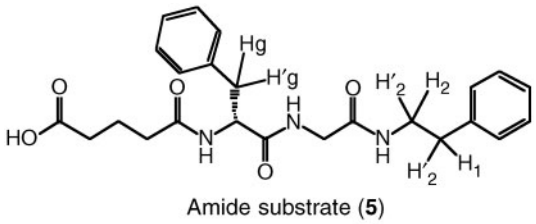

Amide substrate (**5**)

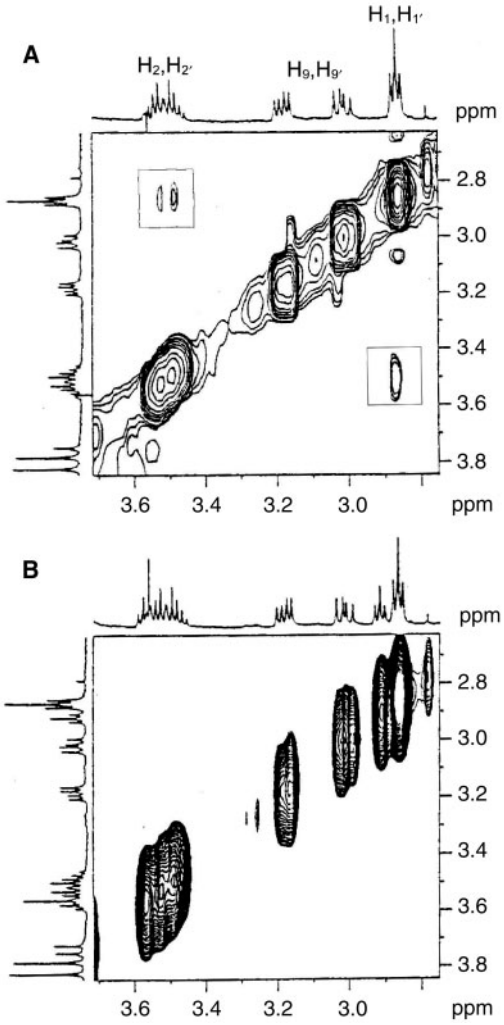

Fig. 9. **NOESY of amide substrate (5) and non-catalytic antibody BS6-16.** The trNOE signals are shown in the frames in (**A**), which disappeared in the presence of 80 μM of TSA **4** (**B**). NOESY shown in (**A**) and (**B**) were obtained at mixing time of 200 ms.

biomolecule are labelled with information of the large proteins (*44*). The large negative NOEs reach their maximal at shorter mixing times (*44*).

The NOESY spectrum shown in Figs. 9A and 10A were recorded after addition of amide substrate (**5**) (Fig. 9) or Product-B (**3**) (Fig. 10) to BS6-16 antibody solution. The spectra show that methylene protons between (H_1, H'_1) and (H_2, H'_2) of the phenethyl group in amide substrate (**5**) or Product-B (**3**) give rise to a negative signal of trNOEs at a mixing time of 200 ms. NOESY reference spectra of amide substrate (**5**) and

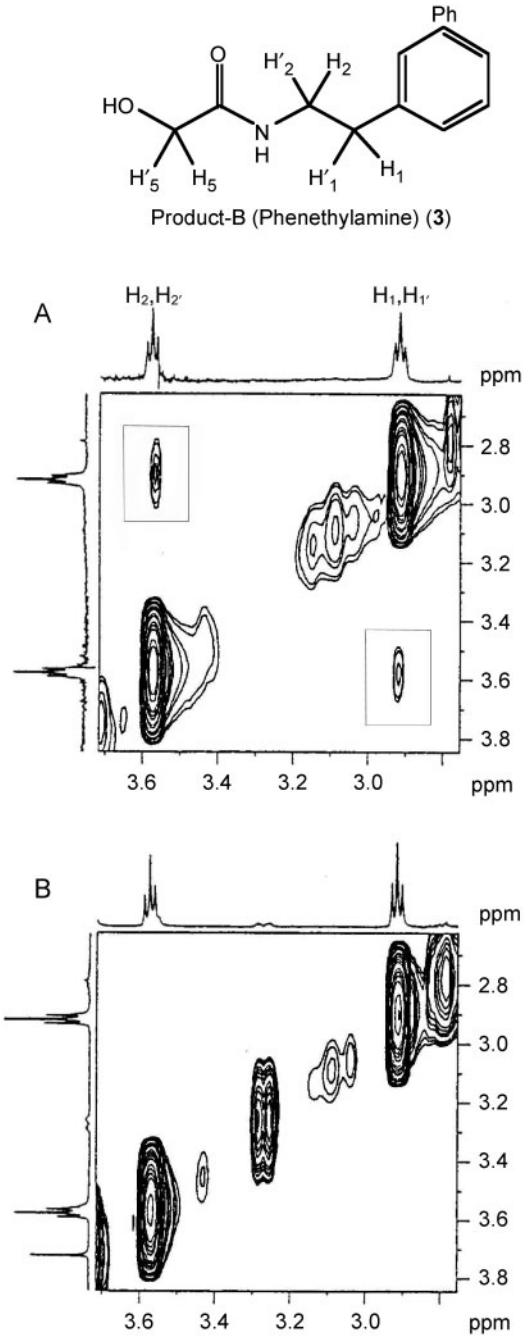

Fig. 10. **NOESY of Product-B (3) and non-catalytic antibody BS6-16.** The trNOE signals are shown in the frames in (**A**), which disappeared in the presence of 80 μM of TSA **4** (B). NOESY shown in (**A**) and (**B**) were obtained at mixing time of 200 ms.

Product-B (**3**) show that even in the absence of BS6-16 antibody methylene protons between (H_1, H'_1) and (H_2, H'_2) of the phenethyl group in amide substrate (**5**) or Product-B (**3**) give rise to a cross-peaks of the small positive signal of NOEs (data not shown). The NOESY spectra shown in Figs. 9B and 10B were recorded after addition of amide substrate (**5**) (Fig. 9) or Product-B (**3**) (Fig. 10) to BS6-16 antibody in the presence of 80 μM of TSA (**4**) at an equivalent concentration of the antibody solution. The spectra show that

Table 3. **TrNOE siganls observed on different mixing times.**

Ligand/Antibody	Mixing time (ms)				
	100	200	400	600	200[a]
Amide-substrate (**5**)/MS6-164	–	–	–	–	NE[d]
Amide-substrate (**5**)/BS6-16	–	+[b]	+	+	–[b]
Product-A (**2**)/MS6-164	–	–	–	–	NE[d]
Product-A (**2**)/BS6-16	–	–	–	–	NE[d]
Product-B (**3**)/MS6-164	–	–	–	–	NE[d]
Product-B (**3**)/BS6-16	+	+[c]	NE[d]	NE[d]	–[c]

[a]TrNOE experiments in the presence of TSA (**4**). [b]Experimental data are shown in Fig. 9. [c]Experimental data are shown in Fig. 10. [d]NE, not examined.

the trNOE signals of methylene protons between (H_1, H'_1) and (H_2, H'_2) of phenethyl group in amide substrate (**5**) or Product-B (**3**) had disappeared.

In summary, the only trNOE signals observed in BS6-16 antibody in the presence of amide substrate were those of methylene protons between (H_1, H'_1) and (H_2, H'_2) of the phenethyl group of amide substrate (**5**) at mixing times from 200 to 600 ms. This was also the case for BS6-16 antibody in the presence of Product-B (**3**) at mixing times of 100–200 ms (data were not obtained at 400–600 ms). No trNOEs were observed in MS6-164 antibody in the presence of either amide substrate (**5**) or Product (B) (**3**) (Table 3).

X-ray crystallography—Analysis of a crystal formed from a binary complex of MS6-164 and TSA (**4**) solved the structures of the Fab fragment of MS6-164 antibody (*47*). We calculated the ESP of MS6-164 Fab with the TSA (**4**) in the combining site (active site) from the atom coordinates of the solved structure. The calculated ESP is shown on a semi-transparent solvent accessible surface (1.4 Å probe radius) (Fig. 11).

One of the striking results of this study is the finding of a strong and large positive ESP spreading around the LysH95. This indicates that there is a strong coulomb interaction between the amino group of LysH95 and the oxyanion(s) of the phosphonate group in TSA (**4**). Fig. 11A and B also show that this positively charged surface region around LysH95 is located just around the mouth of the deep pocket cavity, where the terminal phenethyl group of TSA (**4**) resides.

DISCUSSION

An important feature of catAbs is the presence of amino acid residues that participate in the chemical reaction at the substrate-combining site (catalytic site or active site). For esterolytic antibodies, positively charged residues should be placed in the centre of the combining site. It is believed that those residues complementarily to the transition-state of the substrate would facilitate the stabilization of the 'oxyanion-hole'. Nevertheless, there is no direct evidence so far for what the catalytic residue(s) really does to the substrate and its transition-state. Two antibodies, an esterolytic catAb (MS6-164) and a non-catAb (BS6-16), both of which were elicited and selected against TSA (4) (*20*, *45*), were chosen for comparison to reveal the interaction between the

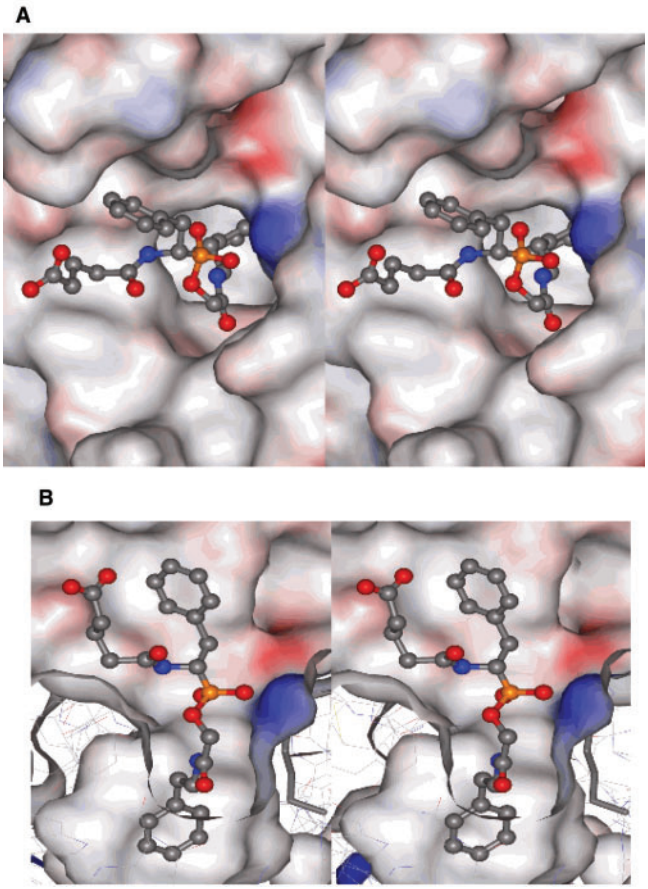

Fig. 11. **A stereo diagram of EPS on the semi-transparent solvent accessible surface (1.4 Å probe radius) that shows interaction of catalytic pocket of MS6-164 and TSA (4).** Coloured in blue are positive EPSs, coloured in red are negative EPSs and coloured in grey are non-charged surfaces. (**A**), plane view from a mouth of the binding pocket; (**B**), elevation view from a side of the binding pocket.

antibodies and its non-cleavable substrate (a mimic of ester substrate) and so forth in reality.

A 3D study of the binary complex with MS6-164 antibody and TSA (**4**) demonstrated the importance of the catalytic residues in the combining site (LysH95 and HisL91), both of which can form hydrogen bonds with oxygens in the phosphonate (*47*). The findings of the 3D study are consistent with the proposed mechanism of ester hydrolysis for these esterolytic catAbs. The catalytic residues seems to function to stabilize the 'oxyanion hole', which stabilizes the transition-state structure of the ester substrate (**1**) in the case for the hydrolysis of esters (*18*, *19*).

The K_m (which is almost equal to K_s) of MS6-164 antibody for ester substrate (1) is 2.8 μM by ELISA (*20*). This value was the same order of magnitude as the K_d values measured in this study by SPR analysis for the interactions between the amide substrate (**5**) and MS6-164 or BS6-16 (11.7 μM and 11.3 μM, respectively). This suggests that amide substrate (**5**) is an appropriate substitute for evaluating the kinetics of these antibodies. However, even though the K_d values of amide substrate (**5**) for the two antibodies are similar, the on- and off-rate constants are quite different. Both the on- and off-rate constants of MS6-164 were about 1/5 of those of BS6-16. This means that amide substrate (**5**) is held five times longer in the combining site of MS6-164 antibody than in the combining site of BS6-16 antibody. It would seem that the ratios of the on- and/or off-rates of the products would be similar. However, we were unable to measure these rates by the SPR analyses. These K_d values are probably outside the lowest range of values that can be detected by the SPR analysis. In previous studies (*20*, *22*), the K_d values for a compound similar to Product-A (**2**) measured by ELISA, were five orders of magnitude weaker than the K_d values for TSA (**4**). For TSA (**4**), we were also unable to obtain K_d values by SPR analyses. This was probably because TSA (**4**) strongly bound to both antibodies, as revealed by SPR analysis using the BIAcore system. Of all the haptens, TSA (**4**) bound most strongly, and hardly any was released from the antibodies. In previous ELISA measurements, these values were found to be at the level of several tens to hundreds picomoles by a competitive ELISA method (*20*, *22*).

The STD NMR experiments confirmed that Product-B (**3**) interacts with the binding pocket of both the MS6-164 and BS6-16 antibodies. As almost all ^{1}H proton signals of Product-B (**3**) were observed in the STD experiment with short irradiation times, almost all groups of Product-B (**3**) interacted with the binding pocket of both antibodies. On the other hand, the interaction between Product-A (**2**) and its binding sites in the antibodies did not induce a detectable STD signal. Amide substrate (**5**) produced an STD signal in the presence of BS6-16 antibody, but not in the presence of MS6-164 antibody. Addition of TSA (**4**) to the BS6-16 solution in the presence of amide substrate (**5**) completely quenched the STD signals. This suggests that the binding site was structurally specific to the substrate, the amide substrate and the TSA. The failure to observe an STD signal in the reaction mixture of MS6-164 and amide substrate (**5**) is not due to an absence of an interaction between them, because in addition to the crystallographic study, the SPR analysis showed that it interacted with the appropriate K_d value. The absence of STD signal also did not seem to be due to exchange rates from unbound- to bound-state or bound-to unbound-state that were too fast. The last and most plausible explanation for these results is that the exchange rates were too slow to produce an STD signal with saturation times below 1,000 ms.

A NOESY spectrum contains information about the magnetization transfer due to the NOE between all pairs of neighbouring protons in the small molecule (ligand or substrate <1.5 kDa). In the unbound form, the small molecule is generally characterized by short correlation times, where the NOEs are positive signals, or at the boundary of the extreme narrowing limit, where the NOEs approach zero. When such a molecule is bound to the protein, it is characterized by the long correlation time of the protein, where the NOEs are large and negative signals. When the molecule is bound weakly and exchanges between the bound- and free-states at reasonable rates, it produces a detectable intramolecular trNOEs. Intra-molecular signals are said to provide the

best technique for demonstrating the bound-state of the small molecule (*34*, *35*).

The trNOE cross peak signals of methylene protons between (H_1, H'_1) and (H_2, H'_2) of the phenethyl groups of both amide substrate (5) and Product-B (3) were observed in the presence of BS6-16. These cross peak signals were also observed in amide substrate (5) and Product-B (3) in their free states, although the signals were positive in these cases. Essentially, no conformational changes occurred between free- and bound-states. The present trNOE signals suggest that the methylenes of the phenethyl group in amide substrate (5) and in Product-B (3) do not change their relative conformations, and that both bind to the BS6-16 combinding site with the appropriate exchange rates. These interactions were structurally specific because the signals were quenched after addition of TSA (4). No trNOEs were observed in MS6-164 antibody in the presence of either amide substrate (5) or Product (B) (3).

Theoretical considerations may help to explain trNOE signals in the NOESY experiments. The k_{on} and k_{off} rates of a ligand should be larger than the cross-relaxation rates of the ligand protons in both the free- and bound-states. In 2D NOESY experiments, sizable trNOE signals can be observed as long as the ligand molecules can associate with the binding protein and dissociate from the complex at least a few times during the NOE mixing time. As shown by a theoretical simulation, when the ligand off-rate is approximately equal to the inverse of the NOE mixing time (5–10 s^{-1}or $\tau_m = 100–200$ ms), the trNOE signals become observable. However, when the off-rate is slow relative to the inverse of the NOE mixing time, the signal should be much weaker or even non-observable (*48*). Because the exchange off-rates may depend on pH, salt concentration and temperature (*48*), it is difficult to accurately predict the complete answer to the relation between the off-rate of the ligand from the protein and the mixing time. However, trNOE signals can reveal whether the exchanges of interactions are faster or slower.

Based on the present SPR data, the k_{off} rate of amide substrate (**5**) was 0.0625 s^{-1} for MS6-164 antibody and 0.328 s^{-1} for BS6-16 antibody. The mixing time used in these trNOESY experiments for amide substrate (**5**) was 100–600 ms. Thus, the inverse of the mixing time was 1.7–10 s^{-1}. This calculation suggests that the off-rate of amide substrate (**5**) for BS6-16 antibody was still about one-fifth that of the lowest inverse mixing time, but that its off-rate for MS6-164 antibody was far smaller, only 1/25 that of the lowest inverse mixing time.

In summary, the present result suggests that the lower on-rate in the catAb could compensate for the lower off-rate. As a result, the K_d (off-rate/on-rate) values of the catAb become comparable to those of the non-catAb. This results in high affinity for the TSA, which makes it possible to select the catAbs in a large population of non-catAbs.

The EPS on the MS6-164 antibody contains a large and strong positive charge distributed over the LysH95. This strongly positive EPS is located around the center of the combining site, *i.e.* the mouth of the hydrophobic pocket in the cavity, where TSA (**4**) binds its phosphonate group. This region appears to interact by coulomb–coulomb interaction with the negatively charged region, mainly oxyanion(s) of the phosphonate group in TSA (**4**) and the substrate as well. This coulomb–coulomb interaction could influence the on-rate and/or off-rate between antibody and substrate/products or even the TSA. Without the positively charged region in the combining site, such an effect would not be detected.

Based on the above considerations, we propose a model for what a catalytic residue(s), which is thought to play a role to stabilize an 'oxyanion hole', has really to do in the combining site of esterolytic catAbs.

In a theoretical view, interaction between the combining site and its ligand is more affected by off-rate, but less by on-rate, because the on-rate depends much on the stochastic phase (concentrations), while the off-rate depends on the non-stochastic phase (structurally related interactions). In this model, however, a positively charged residue(s) functions to interfere with the interaction between a substrate in its ground-state and a combining site in a catAb at on-rate. It resulted in lowering the on-rate. And once a substrate is placed in the right position, the combining site would hold it for long time enough to allow it to convert a ground-state to a transition-state until they reach an equilibrium between a ground-state and a transition-state (lowering the off-rate). Such an interaction, therefore, would influence both the on-rate as well as off-rate.

Here, we classify the antibodies into four categories in terms of their on- and off-rate constants for a phosphonate TSA; a class with both high on-rate and off-rate (high on/high off-class), both low on-rate and off-rate (low on/low off-class), high on-rate but low off-rate (high on/low off-class) and low on-rate but high off-rate (low on/high off-class).

If antibodies have positively charged amino acid residues at the combining site, these residues strongly interfere the binding of the phosphonate TSA to the combining site due to charge interactions. Such antibodies have a strong disadvantage for selection based on their affinity for a phosphonate TSA, because this interference could reduce the on-rate of the TSA hapten to the antibody. Thus, such an antibody is classified into either a low on/low off-class or a low on/high off-class. Low on/high off-class antibodies cannot be competitive in affinity selection, i.e. it will be readily segregated from the other binders of a high on/low off-class during the course of selection. However, if an antibody belongs to a low on/low off-class or high on/low off-class, it can survive the affinity selection, because the resulting K_d can be low enough for the antibody to be selected.

Catalysts should have a binary nature, binding to both a ground-state and a transition-state. Ideally, selecting strategy, therefore, should be considered in two steps, the first is selecting the binders at a high on-rate against the substrate (or a stable substrate mimic) and then, that is followed by counter-selecting against the TSA at a low off-rate (low off-rate to the TSA), or vice versa. However, such a stepwise selection will be impractical and almost unlikely, once a complementary structure to the TSA is formed in a combining site. An alternative strategy of one-step panning with the TSA is the off-rate driven and

has advantage to choose the species with a high on-rate/low off-rate to the TSA. As the species with the high on-rate/low off-rate to the TSA are not to be a catalyst at all, they must be exclusively eliminated among the low off-rate binders to the TSA. In a method named, 'on-and/or off-rate' driven *in vitro* selection method of catAbs, as the stage of binding to the TSA before reaching the binding saturation (k_{on} phase), the antibodies that show the low on-rates exchanges can be collected as those that do not bind to the TSA well. At the stage of release of the TSA from antibodies (k_{off} phase), the antibodies that show the low-off rates exchanges can be collected as those that bind to the TSA well. After repeating these cycles, the number of the antibodies with low on- and off-rates exchanges can be enriched at high concentrations.

Extrapolating this model to general natural catalysts, we can understand the way how catalysts evolve from molecules that non-catalytically bind to the substrate. Molecules that did not have enough complementary residues at the combining site to stabilize the interaction with the substrate would bind to the substrate with high on- and off-rates. Such 'fast-exchange binders' would have little chance of being selected as catalysts. But molecules that bind to the substrate with low on- and off-rates, 'slow exchange binders', have a greater chance of being selected as catalysts because they would hold the substrate for a long enough time to find in the catalytic site the right residues that convert the ground-state of substrate into a transition-state.

We thank the support staff at the Laboratory of Life Science and Biomolecular Engineering, Japan Tobacco, Inc. for preparing the transition-state analogue, substrate, products and preparing monoclonal antibodies used in this experiment. We thank the supporting staff at CCLRC Daresbury Laboratory for assistance with station alignment. We are grateful to Dr Masashi Miyano (RIKEN Harima Institute, Sayo-gun, Hyogo, Japan) for valuable advice on Fab preparation.
This work was supported by the New Energy and Industrial Technology Development Organization as an R & D project of Industrial Science and Technology Frontier Program of Japan, the British Council, BBSRC and the Wellcome Trust. The Krebs Institute is a designated BBSRC Biomolecular Science Center and a member of the North of England Structural Biology Center.

REFERENCES

1. Pauling, L. (1948) Chemical achievement and hope for the future. *Am. Sci.* **36**, 51–58
2. Jencks, W.P. (1969) Catalysis in Chemistry and Enzymology. *Series in Advanced Chemistry,* p. 288, McGraw-Hill, New York
3. Tramontano, A., Janda, K.D., and Lerner, R.A. (1986) Catalytic antibodies. *Science* **234**, 1566–1570
4. Pollack, S.J., Jacobs, J.W., and Schultz, P.G. (1986) Selective chemical catalysis by an antibody. *Science* **234**, 1570–1573
5. Blackburn, G.M., Datta, A., Denham, H., and Wentworth, P. Jr. (1998) Catalytic antibodies. *Adv. Phys. Org. Chem.* **31**, 249–392
6. Lesley, S.A., Patten, P.A., and Schultz, P.G. (1993) A genetic approach to the generation of antibodies with enhanced catalytic activities. *Proc. Natl Acad. Sci. USA.* **90**, 1160–1165
7. Guo, J., Huang, W., and Scanlan, T.S. (1994) Kinetic and mechanistic characterization of an efficient hydrolytic antibody: evidence for the formation of an acyl intermediate. *J. Am. Chem. Soc.* **116**, 6062–6069
8. Zemel, R., Schindler, D.G., Tawfik, D.S., Eshhar, Z., and Green, B.S. (1994) Differences in the biochemical properties of esterolytic antibodies correlate with structural diversity. *Mol. Immunol.* **31**, 127–137
9. Zhou, G.W., Guo, J., Huang, W., Fletterick, R.J., and Scanlon, T.S. (1994) Crystal structure of a catalytic antibody with a serine protease active site. *Science* **265**, 1059–1064
10. Charbonnier, J.-B., Carpenter, E., Giant, B., Golonelli-Pinpaneau, B., Eshhar, Z., Green, B.S., and Knossow, M. (1995) Crystal structure of the complex of a catalytic antibody Fab fragment with a transition state analog: structural similarities in esterase-like catalytic antibodies. *Proc. Natl Acad. Sci. USA.* **92**, 11721–11725
11. Patten, P.A., Gray, N.S., Yang, P.L., Marks, C.B., Wedemayer, G.J., Boniface, J.J., Stevens, R.C., and Schultz, P. (1996) The immunological evolution of catalysis. *Science* **271**, 1086–1091
12. Wedemayer, G.J., Patten, P.A., Wang, L.H., Schultz, P.G., and Stevens, R.C. (1997) Structural insights into the evolution of an antibody combining site. *Science* **276**, 1665–1669
13. Charbonnier, J.-B., Gigant, B., Gollinelli-Pimpaneau, B., and Knossow, M. (1997) Similarities of hydrolytic antibodies revealed by their X-ray structures: a review. *Biochemie* **79**, 653–660
14. Charbonnier, J.-B., Gollinelli-Pimpaneau, B., Knossow, M., Gigant, B., Tawfik, D.S., Chap, R., Schindler, D.G., Kim, S.–H., Green, B.S., Eshhar, Z., and Knossow, M. (1997) Structural convergence in the active sites of a family of catalytic antibodies. *Science* **275**, 1140–1142
15. Wade, H. and Scanlon, T.S. (1997) The structural and functional basis of antibody catalysis. *Biophys. Biomol. Struct.* **26**, 461–493
16. Hilvert, D., MacBeath, G., and Shin, J.A. (1998) The structural basis of antibody catalysis. *Bioorg. Chem. Pept.* **00**, 335–366
17. Wentworth, P. Jr and Janda, K.D. (2001) Catalytic antibodies: structure and function. *Cell Biochem. Biophys.* **35**, 63–87
18. MacBeath, G. and Hilvert, D. (1996) Hydrolytic antibodies: variations on a theme. *Chem. Biol.* **3**, 433–445
19. Tantillo, D.J. and Houk, K.N. (2001) Canonical binding arrays as molecular recognition elements in the immune system: tetrahedral anions and the ester hydrolysis transition state. *Chem. Biol.* **8**, 535–545
20. Takahashi, N., Kakinuma, H., Hamada, K., Shimazaki, K., Takahashi, K., Niihata, S., Aoki, Y., Matsushita, H., and Nishi, Y. (1999) Efficient screening for catalytic antibodies using a short transition-state analog and detailed characterization of selected antibodies. *Eur. J. Biochem.* **261**, 108–114
21. Takahashi, N., Kakinuma, H., Hamada, K., Shimazaki, K., Yamasaki, Y., Matsushita, H., and Nishi, Y. (2000) Improved generation of catalytic antibodies by MRL/MPJ-lpr/lpr autoimmune mice. *J. Immunol. Methods* **235**, 113–120
22. Sun, J., Takahashi, N., Kakinuma, H., and Nishi, Y. (2001) Molecular evolution of catalytic antibodies in autoimmune mice. *J. Immunol.* **167**, 5775–5785
23. Nishi, Y. (2002) Improved generation of catalytic antibodies by MRL/MPJ-lpr/lpr autoimmune mice. *J. Immunol. Methods* **235**, 213–233
24. Nishi, Y. (2002) Evolution of catalytic antibody repertoire in autoimmune mice. *J. Immunol. Methods* **269**, 213

25. Ruzheinikov, S., Muranova, T.A., Sedelnikova, S.E., Partridge, L.J., Blackburn, G.M., Murray, I.A., Kakinuma, H., Takahashi-Ando, N., Shimazaki, K., Sun, J., Nishi, Y., and Rice, D.W. (2003) High-resolution crystal structure of the Fab-fragments of a family of mouse catalytic antibodies with esterase activity. *J. Mol. Biol.* **332**, 423–435
26. Reid, D.G., Salisbury, S.A., and Williams, D.H. (1983) Proton nuclear Overhauser effect study of the structure of an actinomycin D complex with a self-complementary tetranucleoside triphosphate. *Biochemistry* **22**, 1377–1385
27. Poppe, L., Brown, G.S., Philo, J.S., Nikrad, V., and Shah, B.H. (1997) Conformation of slyx tetrasaccharide, free in solution and bound to E-, P-, and L-selectin. *J. Am. Chem. Soc.* **119**, 1727–1736
28. Mayer, M. and Meyer, B. (1999) Characterization of ligand binding by saturation transfer difference NMR spectroscopy. *Angew. Chem. Int. Ed.* **38**, 1784–1788
29. Klein, J., Meinecke, R., Mayer, M., and Meyer, B. (1999) Detecting binding affinity to immobilized receptor proteins in compound libraries by HR-MAS STD NMR. *J. Am. Chem. Soc.* **121**, 5336–5337
30. Vogtherr, M. and Peters, T. (2000) Application of NMR based binding assays to identify key hydroxy groups for intermolecular recognition. *J. Am. Chem. Soc.* **122**, 6093–6099
31. Haselhorst, T., Weimar, T., and Peters, T. (2001) Molecular recognition of sialyl Lewis X and related saccharides by two lectins. *J. Am. Chem. Soc.* **123**, 10705–10714
32. Mayer, M. and Meyer, B. (2001) Group epitope mapping by saturation transfer difference NMR to identify segments of a ligand in direct contact with a protein receptor. *J. Am. Chem. Soc.* **123**, 6108–6117
33. Benie, A.J., Moser, R., Bäuml, E., Blaas, D., and Peters, T. (2003) Virus-ligand interactions: identification and characterization of ligand binding by NMR spectroscopy. *J. Am. Chem. Soc.* **125**, 14–15
34. Balaram, P., Bothner-By, A.A., and Dadok, J. (1972) Negative nuclear Overhuaser effects as probes of macromolecular structure. *J. Am. Chem. Soc.* **94**, 4015–4017
35. Balaram, P., Bothner-By, A.A., and Dadok, J. (1972) Localization of tyrosine at the binding site of neurophysin II by negative nuclear Overhouser effects. *J. Am. Chem. Soc.* **94**, 4017–4018
36. Cooke, R.M., Hale, R.S., Lister, S.G., Shah, G., and Weir, M.P. (1994) The conformation of the sialyl Lewis X ligand changes upon binding to E-selectin. *Biochemistry* **33**, 10591–10596
37. Scheffler, L., Ernst, B., Katopodis, A., Magnani, J.L., Wang, W.T., Weisemann, R., and Peters, T. (1995) Determination of the bioactive conformation of the carbohydrate ligand in the E-selectin/sialyl Lewis complex. *Angew. Chem. Int. Ed. Engl.* **34**, 1841–1844
38. Shuker, S.B., Hajduk, P.J., Meadows, R.P., and Fesik, S.W. (1996) Discovering high-affinity ligands for proteins: SAR by NMR. *Science* **274**, 1531–1534
39. Jahnke, W., Kolb, H.C., Blommers, M.J.J., Magnani, J.L., and Ernst, B. (1997) Comparison of the bioactive conformations of sialyl Lewis X and a potent sialyl Lewis X mimic. *Angew. Int. Ed. Engl.* **36**, 2603–2607
40. Meyer, B., Weimar, T., and Peters, T. (1997) Screening mixtures for biological activity by NMR. *Eur. J. Biochem.* **246**, 705–709
41. Driggers, E.M., Cho, H.S., Liu, C.W., Katzka, C.P., Braisted, A.C., Ulrich, H.D., Wemmer, D.E., and Schultz, P.G. (1998) Mechanistic studies of an antibody-catalysed pericyclic rearrangement. *J. Am. Chem. Soc.* **120**, 1945–1958
42. Driggers, E.M., Liu, C.W., Wemmer, D.E., and Schultz, P.G. (1998) Structure of the Michaelis complex of an efficient antibody acyl transferase determined by transferred nuclear Overhauser enhancement spectroscopy. *J. Am. Chem. Soc.* **120**, 7395–7396
43. Haselhorst, T., Espinosa, J.-F., Jiménez-Barbero, J., Sokolowski, T., Kosma, P., Brade, H., Brade, L., and Peters, T. (1999) NMR experiments reveal distinct antibody-bound conformations of a synthetic disaccharide representing a general structural element of bacterial lipopolysaccharide epitopes. *Biochemistry* **38**, 6449–6459
44. Mayer, M. and Meyer, B. (2000) Mapping the active site of angiotensin-converting enzyme by transferred NOE spectroscopy. *J. Med. Chem.* **43**, 2093–2099
45. Kakinuma, H., Shimazaki, K., Takahashi, N., Takahashi, K., Niihata, S., Aoki, Y., Hamada, K., Matsushita, H., and Nishi, Y. (1999) Comparison of phosphonate transition state analogs for inducing catalytic antibodies and evaluation of key structural factors by an ab initio study. *Tetrahedron* **55**, 2559–2572
46. Muranova, T.A., Ruzheinkov, S.N., Sedelnikova, S.E., Moir, A., Partridge, L.J., Kakinuma, H., Takahashi, N., Shimazaki, K., Sun, J., Nishi, Y., and Rice, D. (2001) The preparation and crystallization of Fab fragments of a family of mouse esterolytic catalytic antibodies and their complexes with a transition-state analogue. *Acta Crystallog.* **Sect. D. 57**, 1192–1195
47. Nishi, Y., Takahashi, N., Kakinuma, H., and Sun, J. (2000) Catalytic antibodies in autoimmune mice. *Chem. Immunol.* **77**, 58–79
48. Ni, F. (1994) Recent developments in transferred NOE methods. *Progress in NMR Spectroscopy* **26**, 517–606